Synthesis, structure and properties of V(III, IV and V) complexes with ONO Schiff bases

Janusz Szklarzewicz*, Anna Jurowska, Agata Olszewska, Maciej Hodorowicz, Ryszard Gryboś, Krzysztof Kruczała

Jagiellonian University, Faculty of Chemistry, Gronostajowa 2, 30-387 Kraków, Poland

Article history:
Received 7 December 2018
Received in revised form
10 March 2019
Accepted 2 April 2019
Available online 3 April 2019

Abstract

The synthesis and physicochemical properties of vanadium(III,IV,V) complexes with Schiff base ligands based on 3,5-dibromo-4-methoxy-salicylaldehyde and phenylacetic hydrazide (H_2L^1), 5-chlorosalicylaldehyde and 4-hydroxybenzhydrazide (H_2L^2) and 5-chlorosalicylaldehyde and 2-hydroxybenzhydrazide (H_2L^3) were presented. The formulas of the complexes {$[V(L_1)(HL^1)]\cdot EtOH$ (**1**), $[VO(L^2)(phen)]\cdot 2H_2O$ (**2**) and $[VO(L^3)(EtO)]$ (**3**)} were proposed based on the elemental analysis, IR and UV-Vis spectra. Additionally, the IR and UV-Vis spectra (in solvents as well as in a solid state) have been discussed from the vanadium oxidation state point of view. The single crystal structure of **3** shows triclinic, P_{-1} space group, structure is stabilized by hydrogen bonds and strong π-π stacking interactions. The oxidation state of the metal centre was also confirmed by the magnetic susceptibility measurements. The stability of the complexes was measured in pH = 7.00 and in pH = 2.00 which allows to evaluate the use of these compounds as insulin mimetic compounds.

Keywords: vanadium, complex, Schiff base, oxidation state, structure, IR, UV-Vis, EPR

Introduction

The biological activity of vanadium compounds with organic ligands is multidirectional – they are known for exhibiting several bioactivities [1-2] and showing potential as pharmaceutical drugs [3]. Vanadium can occur at various degrees of oxidation from -3 to +5 and the state of vanadium in a compound is highly dependent on pH [4], most often as four- and five-valent derivatives, while compounds in the form of trivalent derivatives are unstable in the presence of oxygen under physiological conditions. Thus, in most applications and studies on biological activity vanadium is in form of V(IV) or V(V) salts. It is postulated that cation V(IV) readily oxidizes to V(V) and occurs in living organisms as an anion [5]. At the beginning simple vanadium inorganic salts were used, as vanadyl sulphate or vanadates. In 90's first vanadium(IV) complex with maltolato ligand was synthesized and soon application of more bioactive complexes with organic ligands has started. It is also worth noting that vanadium compounds exhibit large differences between them in terms of their structure and, therefore, show a difference in permeability through the cell membrane to the body. Vanadium derivatives have antidiabetic [6-8], anticancer effects [9-13] and lower blood pressure [14]. What is more, it is said that they show greater activity in comparison to the commonly used anticancer drugs [15]. For many years vanadium compounds have shown also their insulin-enhancing and insulin-mimetic effects in treatment of diabetes [16-17]. Further research on this group of transition metal complexes can lead to progress in improvement of innovative metal-based therapeutic drugs.

In this paper we described the results of the research which aim was to compare vanadium complexes with diverse structures and correlate it with their properties, which is important from the point of view of their subsequent pharmacological application. In reference to these observations, we synthesized a group of vanadium complexes at three different oxidation levels (III, IV and V) showing differences in the coordination of the metal with the ligand in order to compare their physicochemical and spectroscopic properties as potential antidiabetic drugs. The complexes were obtained from different vanadium compounds such as: $[V(acac)_3]$, $[VO(acac)_2]$ and $VOSO_4$ and ONO hydrazine Schiff base ligands derived from 3,5-dibromo-4-methoxy-salicylaldehyde with phenylacetic hydrazide, 5-chlorosalicylaldehyde with the following hydrazides: 4-hydroxybenzhydrazide and 2-hydroxybenzhydrazide. For all of the complexes the elemental analysis, IR, UV-Vis spectra, magnetic susceptibility and cyclic voltammetry, as well as EPR for one of the compounds, are presented.

Materials and Methods

$[V(acac)_3]$, $[VO(acac)_2]$, $VOSO_4$aq, 3,5-dibromo-4-methoxy-salicylaldehyde, 5-chlorosalicylaldehyde, phenylacetic hydrazide, 4-hydroxybenzhydrazide and 2-hydroxybenzhydrazide, 1,10-phenanthroline were of analytical grade (Aldrich) and were used as supplied. Ethanol (98%) of pharmaceutical grade was

*Corresponding author: szklarze@chemia.uj.edu.pl,
tel: 48-12-663-2231, fax: 48-12-634-05-15

from Polmos (Poland) and used as supplied. All other solvents were of analytical grade and were used as supplied. $BaSO_4$ was of spectroscopic grade (Japan). Microanalysis of carbon, hydrogen and nitrogen were performed using Elementar Vario MICRO Cube elemental analyzer. IR spectra were recorded on a Bruker EQUINOX 55 FT-IR spectrophotometer in KBr pellets. The electronic absorption spectra were recorded on Shimadzu UV-3600 UV-Vis-NIR spectrophotometer equipped with a CPS-240 temperature controller. Diffuse reflectance spectra were measured in $BaSO_4$ pellets with $BaSO_4$ as a reference on Shimadzu 2101PC equipped with an ISR-260 integrating sphere attachment. Complex stability measurements in DMSO/H_2O (20 µL/3mL) mixture were performed at a pH = 7.00 and at pH = 2.00 (0.1M KCl, HCl added to adjust the pH). The spectra were measured every 340 s at 36.7 °C on Shimadzu UV-3600 UV-Vis-NIR spectrophotometer in 1 cm UV cuvettes. The magnetic susceptibility measurement was performed on a SHERWOOD SCIENTIFIC magnetic susceptibility balance. The EPR measurements were performed at room and liquid nitrogen temperatures with a Bruker ELEXSYS E-500 spectrometer operating at the X band (9.8 GHz) and 100 kHz magnetic field modulation equipped with super-high-sensitivity cavity ER 4122 SHQE. The EPR parameters of the vanadium complex were determined by fitting the spectra using the EPRSim32 simulation package [18]. The estimated error of the g factor was ±0.001 whereas in the case of HFS parameters the one was ±1 G.

Syntheses

The syntheses of three vanadium(III,IV,V) complexes were carried out in the one step reaction, ethanol was used as a solvent and reactions were proceeding under anaerobic conditions (Ar). The Schiff base ligands were synthesized *in situ* in 1 : 1 molar ratio from components (aldehydes and hydrazides) prior of vanadium source addition. The structure of ligands H_2L^1 – H_2L^3 is presented in Scheme 1.

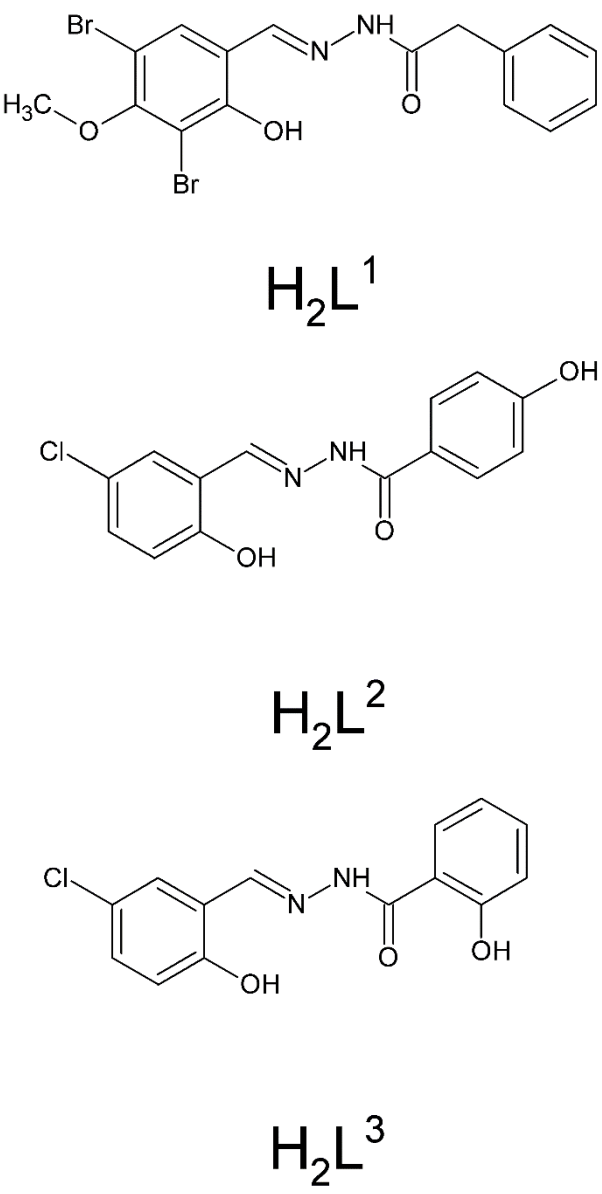

Scheme 1. Structure of ligands H_2L^1 – H_2L^3

[V(L_t)(HL^1)]·EtOH, 1

3,5-dibromo-4-methoxy-salicylaldehyde (0.929 g, 3.0 mmol), phenylacetic hydrazide (0.450 g, 3.0 mmol) and EtOH (25 ml) were refluxed under Ar for 10 minutes. Formation of white precipitation was observed. Then [V(acac)$_3$] (0.590 g, 1.7 mmol) was added and the reflux was continued for 35 minutes. The formation of precipitate (very small amounts) was observed. The mixture was evaporated to ½ of initial volume and the product was filtered off while hot. Yield 1.148 g. MW = 977.18. Anal. Calcd. for $C_{34}H_{31}Br_4N_4O_7V$: C, 41.79; H, 3.09; N, 5.73 %. Found: C, 41.45; H, 2.85; N, 6.03 %. The complex is paramagnetic, µ = 2.55 μ_B.

[VO(L^2)(phen)]·2H_2O, 2

5-chlorosalicylaldehyde (0.234 g, 1.5 mmol), 4-hydroxybenzhydrazide (0.224 g, 1.5 mmol) and EtOH (50 ml) were refluxed under Ar for 10 minutes. The light yellow solution was formed and then solid [VO(acac)$_2$] (0.399 g, 1.5 mmol) was added and the mixture was refluxed for additional 20 minutes. The mixture becomes brown and no crystal formation was observed. Then phen (0.277 g, 1.5 mmol) in 10 ml of EtOH was added. The solution becomes blooded-red and it was left for crystallization, as no precipitation was observed at this stage. The next day formation of crystals was observed. These were filtered off, washed with small amount of cold EtOH and dried in air. Yield 0.514 g. MW = 571.86. Anal. Calcd. for $C_{26}H_{21}ClN_4O_6V$: C, 54.61; H, 3.70; N, 9.80 %. Found: C, 54.54; H, 3.57; N, 9.58 %. The complex is paramagnetic, µ = 1.52 μ_B.

[VO(L^3)(EtO)], 3

5-chlorosalicylaldehyde (0.53 g, 1.5 mmol) and 2-hydroxybenzhydrazide (0.230 g, 1.5 mmol) in 25 ml of EtOH were refluxed

for 15 minutes under Ar. The insoluble Schiff base was formed and solution becomes light yellow. Then $VOSO_4$ aq (0.333 g; 1.5 mmol) was added and reflux was continued for 55 minutes. The solution becomes transparent, very dark yellow without any precipitation. The reflux was removed and the solvent was evaporated but no precipitation was observed. Thus water was added and the mixture was sonicated for several minutes. The complex was filtered off, washed with water 3 times and dried in air. Yield 0.574 g. MW = 400.69. Anal. Calcd. for $C_{16}H_{14}ClN_2O_5V$: C, 47.96; H, 3.52; N, 6.99 %. Found: C, 48.34; H, 3.49; N, 7.05 %. The complex is diamagnetic.

Crystallographic data collection and structure refinement

Diffraction intensity data for single crystal of the compound **3** were collected at a room temperature on a KappaCCD (Nonius) diffractometer with graphite-monochromated Mo Kα radiation (λ = 0.71073 Å). Cell refinement and data reduction were performed using firmware [19, 20]. Positions of all of non-hydrogen atoms were determined by direct methods using SHELXL-2017/1 [21]. All non-hydrogen atoms were refined anisotropically using weighted full-matrix least-squares on F^2. Refinement and further calculations were carried out using SHELXL 2017/1 [21]. All hydrogen atoms joined to carbon atoms were positioned with an idealized geometries and refined using a riding model with $U_{iso}(H)$ fixed at 1.5 U_{eq} of C for methyl groups and 1.2 U_{eq} of C for other groups. The hydrogen atom of -OH (O19) substituent was found in the difference-Fourier map and refined with an isotropic thermal parameter. The figures were made using DIAMOND software [22]. CCDC 1883287 contains the supplementary crystallographic data for the complex. These data can be obtained free of charge from the Cambridge Crystallographic Data Centre via www.ccdc.cam.ac.uk/data_request/cif.

Results and Discussion

The reaction of $[V(acac)_3]$, $[VO(acac)_2]$ or $VOSO_4$aq, in anaerobic conditions, with Schiff base ligand components, listed in materials and methods section, leads to formation of tridentate ONO ligand and for **1** and **2** release of $acac^-$ ions. For V(III) complex (**1**) two Schiff base ligands are coordinated to octahedral vanadium center, one as 2- anion (with deprotonated phenolic OH group of salicylaldehyde imine nitrogen and oxygen from deprotonated hydrazide) and second as 1- anion (with deprotonated phenolic OH group of salicylaldehyde imine nitrogen) for this non-oxido vanadium(III) complex. In case of V(IV) (**2**), when as a substrate a $[VO(acac)_2]$ was used, for stabilization of the IV oxidation state and to fill the coordination sphere to six, bidentate 1,10-phenanthroline was used. Thus octahedral coordination sphere of vanadium(IV) is composed of oxido ligand, ONO twice deprotonated L^2 ligand and two nitrogen donor atoms of phen. When a co-ligand was not added, the compounds were oxidized in the presence of air, yielding V(V) salts as in case of complex **3**. All complexes are stable in air, well soluble in the organic solvents and slightly soluble in water.

1. Crystal structure

The complex **3** crystallizes in the triclinic space group P_{-1} with the asymmetric cell unit containing one molecule of $[VO(L^3)(EtO)]$ complex. The crystallographic data and detailed information on the structure solution and refinement for **3** are given in Table 1 while the molecular structure with the atom labelling scheme is illustrated in Fig. 1. The selected bond parameters are summarized in Table 2. Vanadium is in distorted square pyramidal geometry, with $(L^3)^{2-}$ and EtO^- in pyramid plane. Ligand $(L^3)^{2-}$ is planar, only N9 and O12 are shifted off plane by 0.279 Å and 0.287 Å respectively. This plane form an angle of 3.30 ° with that defined by atoms O7, O12, O21 and N9. Vanadium atom is shifted toward vanadyl oxygen O20 from this last plane by 0.470 Å. This a rear example of pure square pyramid geometry. The V=O distance (1.577 Å) is typical for double bond, the V-N9 (2.115 Å) and V-O (1.758 Å) to EtO^- oxygen bond distances indicate on strong bonding of ethoxy ligand. The V-O7 bond distance (1.829 Å) and V-O12 (1.928 Å) indicate stronger torsions in pentagonal ring than in hexagonal (with O7) one. The EtO^- ligand shows two distinct positions in the structure, as shown in Fig. 1. There are two isomers present in the crystal structure, looking from EtO^- ligand 5-atomic ring is on the left or on the right sight of the molecule. In unit cell, the 1:1 stoichiometry of isomers is observed.

Table 1. Crystal data and structure refinement for **3**

Empirical formula	$C_{16}H_{14}ClN_2O_5V$	
Formula weight	400.68	
Temperature	293(2) K	
Wavelength	0.71073 Å	
Crystal system	Triclinic	
Space group	P -1	
Unit cell dimensions	a = 7.5605(6) Å	α = 90.196(4)°
	b = 8.6791(7) Å	β = 99.341(4)°
	c = 12.9344(8) Å	γ = 98.891(4)°
Volume	827.06(11) $Å^3$	
Z	2	
Density (calculated)	1.609 Mg/m^3	
Absorption coefficient	0.791 mm^{-1}	
F(000)	408	
Crystal size	0.350 x 0.180 x 0.060 mm^3	
Theta range for data collection	2.376 to 27.612°	
Index ranges	-9≤h≤9, -11≤k≤11, -5≤l≤16	
Reflections collected	3734	
Independent reflections	3734 [R(int) = 0.0706]	

Completeness to theta = 25.242°	98.9 %
Refinement method	Full-matrix least-squares on F^2
Data / restraints / parameters	3734 / 4 / 252
Goodness-of-fit on F^2	1.035
Final R indices [I>2sigma(I)]	R1 = 0.0786, wR2 = 0.1923
R indices (all data)	R1 = 0.1157, wR2 = 0.2106
Largest diff. peak and hole	0.666 and -0.647 e.Å^{-3}

Figure 1. The asymmetric part of the unit cell of the complex **3** with adopted atomic numbering scheme. All non-hydrogen atoms are represented at 30% probability thermal ellipsoids

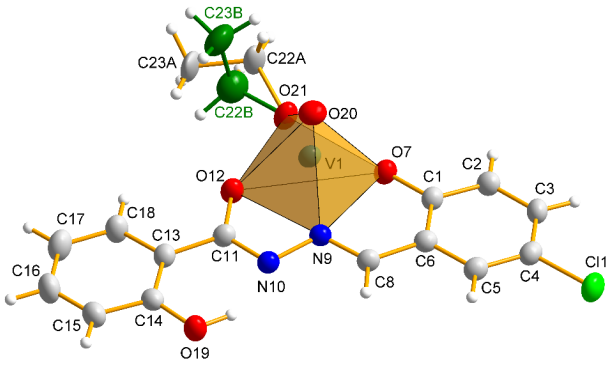

The molecular packing is shown in Fig. 2. The structure is stabilized by a net of hydrogen bonds, shown in Fig. 3 and strong π-π interactions shown in Fig. 4. The numerical data are presented in Table 3 and 4. The D-A distances indicate that hydrogen bonds are relatively long, the DHA angle rather far from 180° indicate that hydrogen bonds are very weak. The structure is stabilized also by π-π stacking interactions listed in Table 4 and shown in Fig. 4. The stacking interaction are in between aromatic rings of ligand L^3. All these interactions form a three-dimensional net that stabilize the structure of **3**.

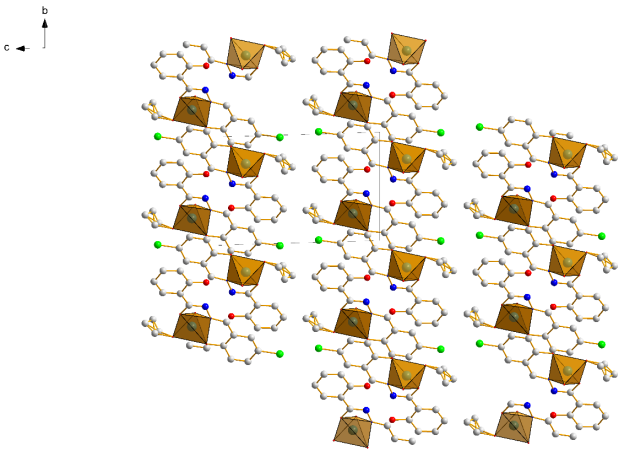

Figure 2. The crystal packing in **3** through [100] direction. Hydrogen atoms omitted for clarity

Table 2. Selected bond lengths [Å] and angles [°] in **3**

Bond lengths		Bond angles	
V(1)-O(20)	1.577(4)	O(20)-V(1)-O(21)	107.5(2)
V(1)-O(21)	1.758(3)	O(20)-V(1)-O(7)	107.56(19)
V(1)-O(7)	1.830(3)	O(21)-V(1)-O(7)	99.62(15)
V(1)-O(12)	1.929(4)	O(20)-V(1)-O(12)	103.89(18)
V(1)-N(9)	2.115(4)	O(21)-V(1)-O(12)	88.94(16)
Cl(1)-C(4)	1.737(5)	O(7)-V(1)-O(12)	142.95(16)
O(21)-C(22A)	1.456(14)	O(20)-V(1)-N(9)	96.87(17)
O(21)-C(22B)	1.457(18)	O(21)-V(1)-N(9)	153.19(18)
O(19)-C(14)	1.356(6)	O(7)-V(1)-N(9)	82.92(14)
O(7)-C(1)	1.355(5)	O(12)-V(1)-N(9)	74.29(14)
O(12)-C(11)	1.315(5)	C(22A)-O(21)-V(1)	130.1(9)
N(9)-C(8)	1.284(6)	C(22B)-O(21)-V(1)	139.4(8)
N(9)-N(10)	1.390(5)	C(1)-O(7)-V(1)	135.0(3)
C(1)-C(6)	1.396(6)	C(11)-O(12)-V(1)	118.6(3)
C(1)-C(2)	1.402(7)	C(8)-N(9)-N(10)	116.2(4)
N(10)-C(11)	1.299(6)	C(8)-N(9)-V(1)	128.7(3)
C(5)-C(4)	1.379(7)	N(10)-N(9)-V(1)	115.1(3)

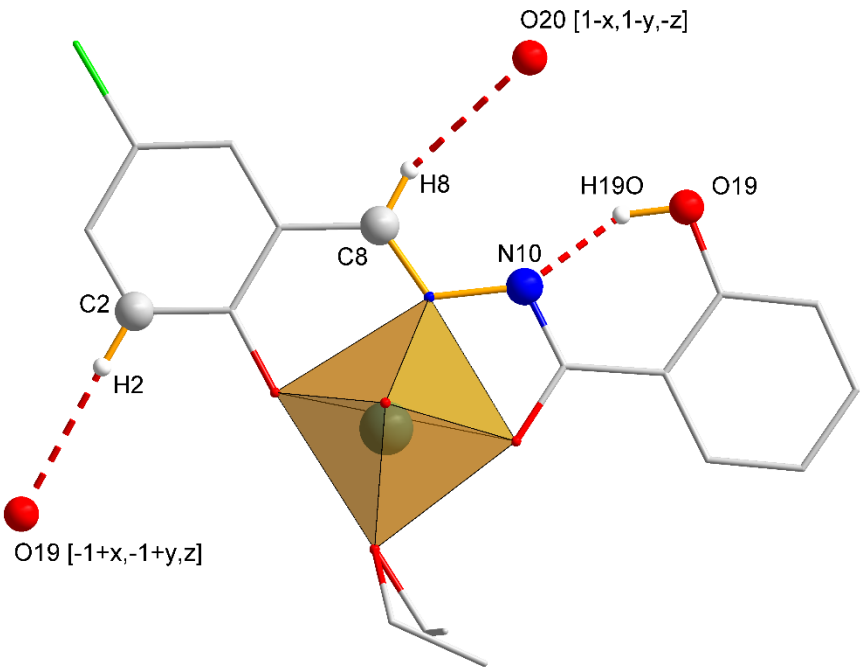

Figure 3. Hydrogen bonds in **3**. H-atoms (without H2, H8 and H19) are omitted for clarity

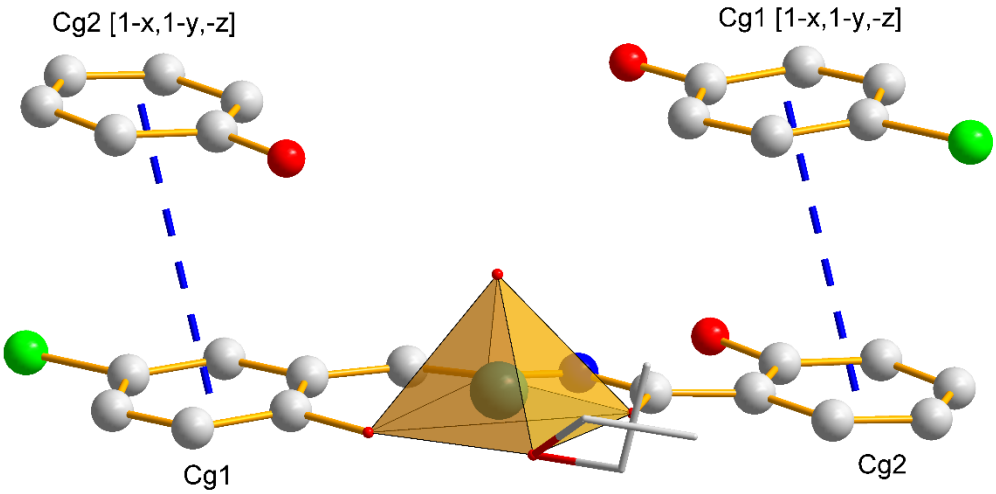

Figure 4. The π-π interactions in **3**. Hydrogen atoms are omitted for clarity

Table 3. Hydrogen bonds [Å] and angles [°] in **3**

D-H...A	d(D-H)	d(H...A)	d(D...A)	<(DHA)
C(8)-H(8)...O(20)#1	0.93	2.59	3.355(6)	139.7
C(2)-H(2)...O(19)#2	0.93	2.50	3.394(6)	161.3
O(19)-H(19O)...N(10)	0.95(2)	1.76(5)	2.614(5)	148(7)

Symmetry transformations used to generate equivalent atoms:
#1 -x+1,-y+1,-z #2 x-1,y-1,z

Table 4. The π···π interactions in **3** [Å]

Cg1····Cg2 [1-X,1-Y,-Z] 3.9518(3)
Cg2····Cg1 [1-X,1-Y,-Z] 3.9518(3)

Cg1: C(1)-C(2)-C(3)-C(4)-C(5)-C(6)
Cg2: C(13)-C(14)-C(15)-C(16)-C(17)-C(18)

2. IR spectra

The infrared spectra for **1-3** were recorded in a 400 – 4000 cm^{-1} range and are presented in Fig. 5. In the region characteristic for V=O vibration (900 – 1000 cm^{-1}) there are bands at 957 cm^{-1} for **2** and at 965 cm^{-1} for **3**. For complex **1** the $\nu_{V=O}$ band does not appear which confirms its non-oxido character. For all complexes the band at 1576 cm^{-1} (for **1**), 1607 cm^{-1} (for **2**) and 1622 cm^{-1} (for **3**) is assigned to the vibration of C=N group in Schiff base ligand. Lower position of this band for **1** may be related to the participation of two nitrogen atoms of imine groups in coordination to the vanadium(III) center. For complex **2** there are also well seen the intensive bands at 724, 1425 and 1493 cm^{-1} connected with the vibration in the 1,10-phenanthroline ligand. These bands were also observed in the other *d*-electron metal

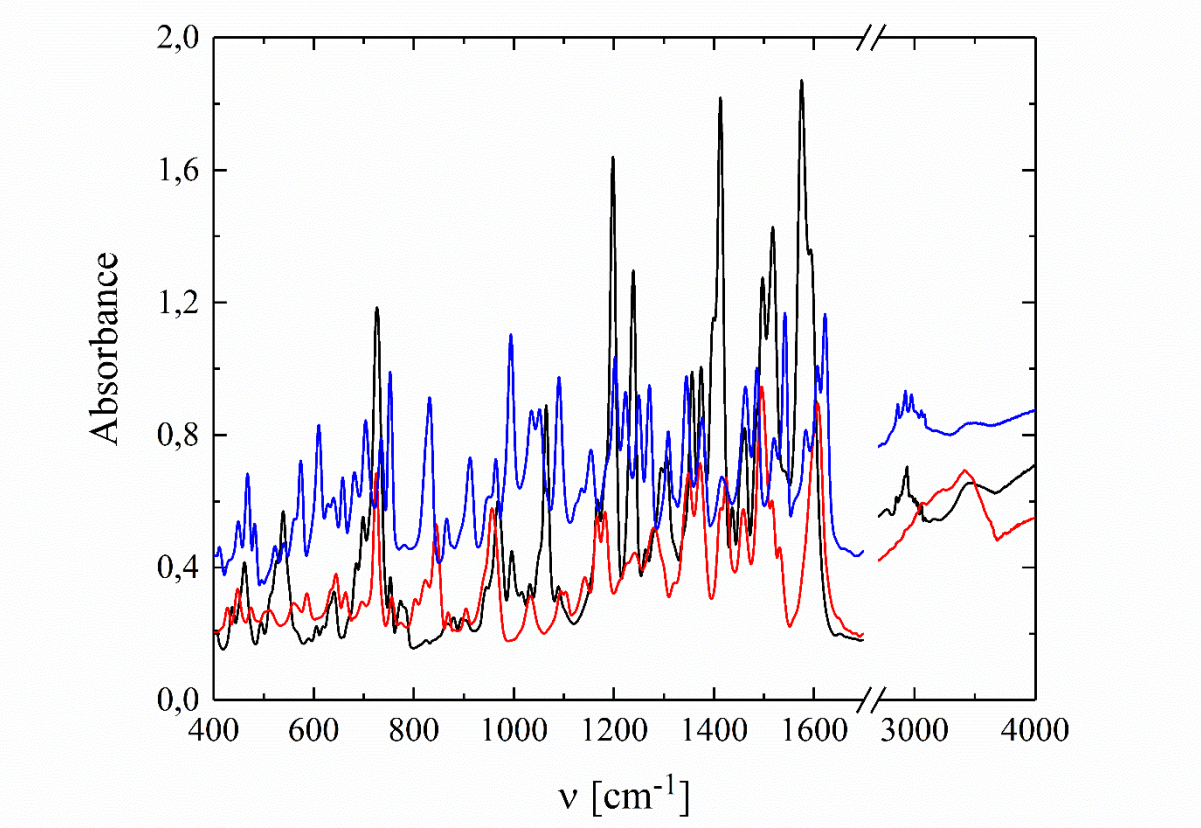

Figure 5. The IR spectra for **1** (black line), **2** (red line) and **3** (blue line)

complexes with 1,10-phenanthroline ligand [23]. For this complex the wide band at 3407 cm^{-1} may be associated with the presence of water of hydration which also stay in agreement with the complex formula. For complexes **1** and **3** there are low intensity bands in a 2800 – 3100 cm^{-1} range and are related to ν_{OH} vibration of EtOH in **1** and EtO^- ligand in **3**. The other parts of the spectra are dominated by bands derived from the organic ligand.

2. UV-Vis spectra

The UV-VIS spectra in 200-800 nm range are presented in Figs. 6-8 for complexes **1-3**, respectively. For complexes **1** and **2** spectra are shown in EtOH and MeCN, while for **3** in several other solvents to indicate the solvatochromism of the CT (charge transfer) band at *ca*. 400 nm which is attributed to MLCT (metal-to-ligand charge-transfer) transition (connected with the coordinated Schiff base ligand). In UV part CT bands of the ligands L^1 – L^3 can be observed. The doubling of the bands in the UV part (in **1**) can be a result of two different forms of protonated ligand, $(HL^1)^-$ and $(L^1)^{2-}$, present in the complex unit. The reflectance spectra of **1** and **3** are presented in Fig. 9. The lack of the bands in the *d-d* region (above 700 nm) underlines the V(III) and V(V) oxidation states in **1** and **3** respectively.

The most important was to study the stability of the complexes in solutions as well as dependence of this stability at different pH. As for biological studies the solutions of complexes have to be prepared, which then were injected to cell cultures, the stability of solutions was crucial. Also the solubility in water was very important. We have found, that all complexes are almost insoluble in water, thus we had to prepare water-organic solvent mixtures. The highest solubility of all complexes was found in DMSO as solvent, thus for this solvent water-DMSO mixtures of lowest organic solvent content could be prepared. We have also found, that solutions in DMSO are very stable in time and mixtures of 20 µl of DMSO complex solution with 3 ml of water could be prepared without complex precipitation. We have studied the stability of such mixtures *versus* time at pH neutral (7.0) and at pH 2.0, this last as representing the medium pH found in human stomach. The results of this investigations are presented in Figs. 10-12. In general most stable are the solutions at pH = 7.0, while at pH = 2 we observed the strong diminishing of the band in 400 nm region indicating complex decomposition with releasing the ONO ligands L.

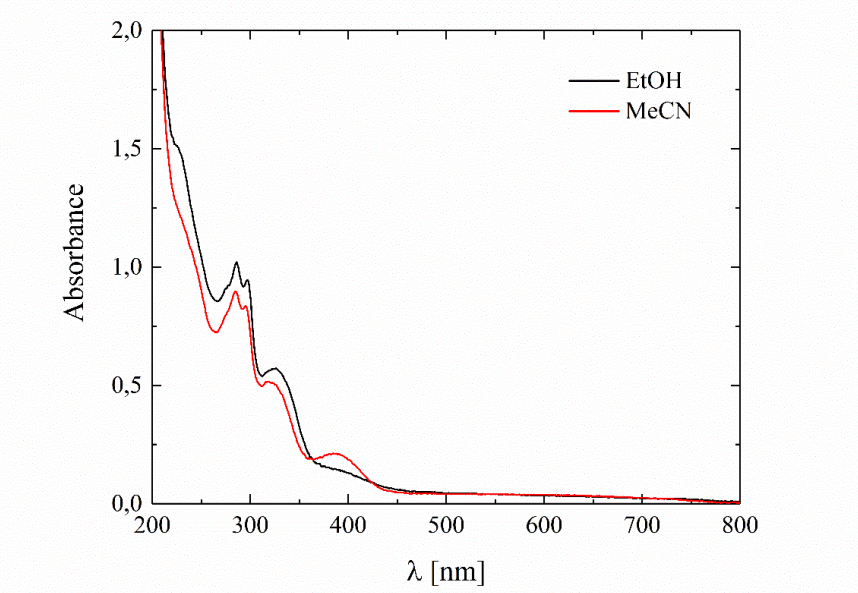

Figure 6. The electron spectra of **1** in ethanol and acetonitrile, d = 1 cm

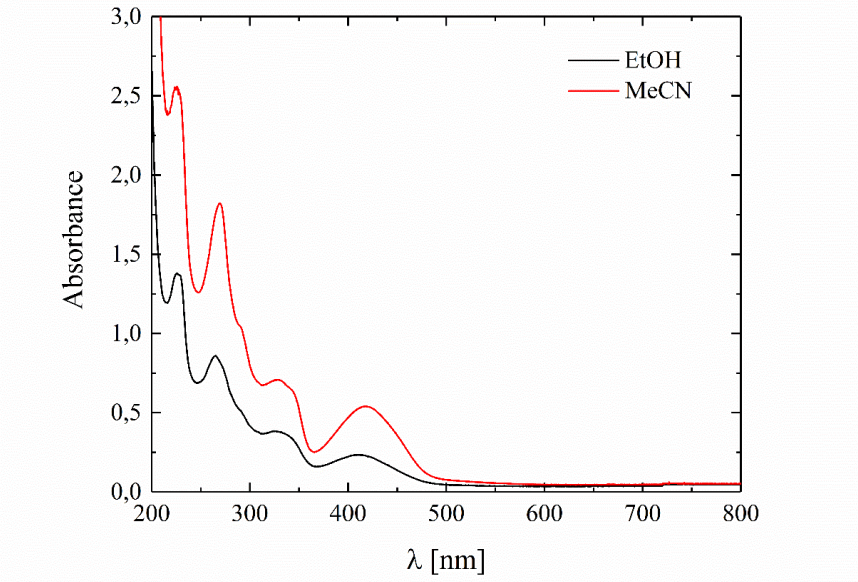

Figure 7. The electron spectra of **2** in ethanol and acetonitrile, d = 1 cm

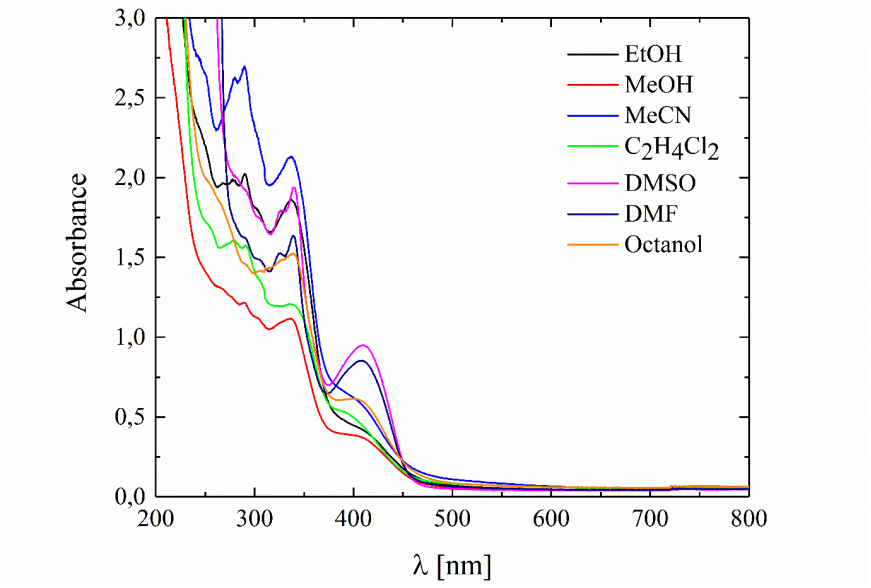

Figure 8. The qualitative electron spectra of **3** in different organic solvents, d = 1 cm

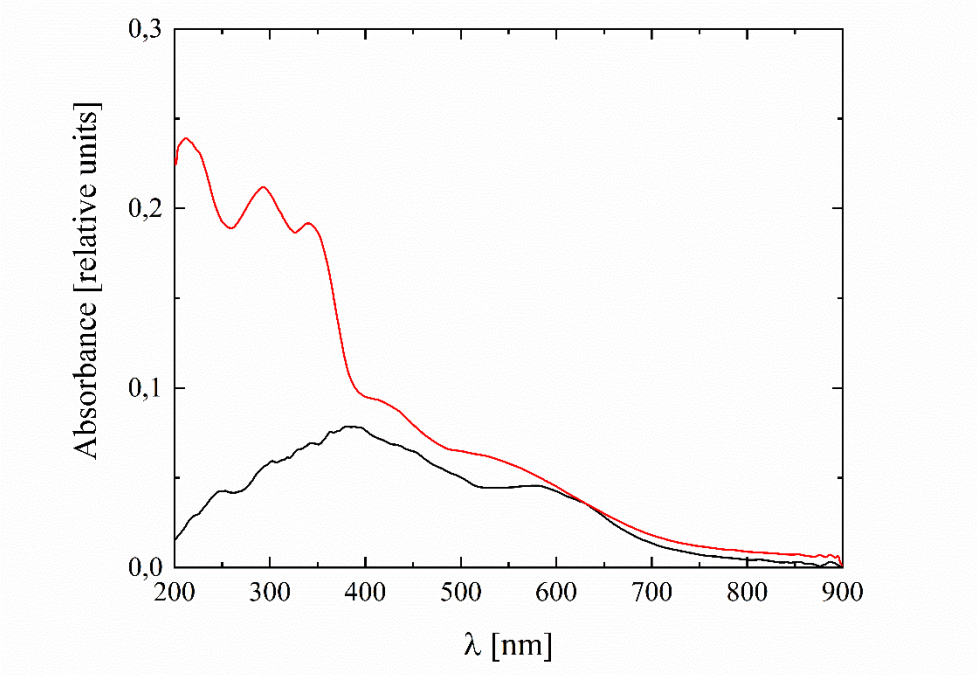

Figure 9. The reflection spectrum of **1** (black line) and **3** (red line) after Kubelka-Munk transformation

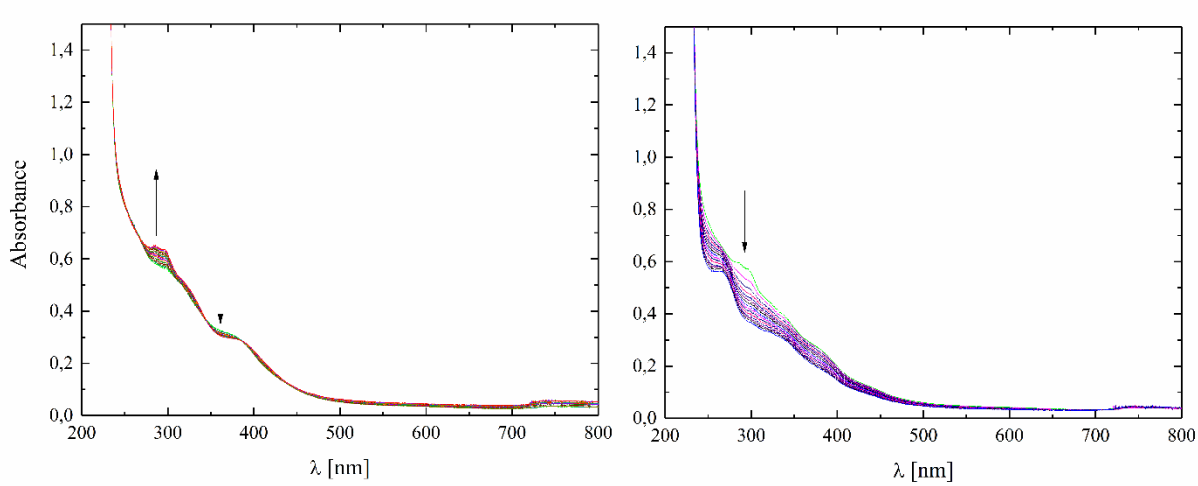

Figure 10. The electron spectra of **1** in DMSO-H_2O mixture (20µl + 3 ml) at pH = 7.00 (left) and 2.00 (right). T = 37°C, d = 1 cm, c = mol/dm^3, 15 spectra measured every 340s. The arrows indicate the direction of the changes

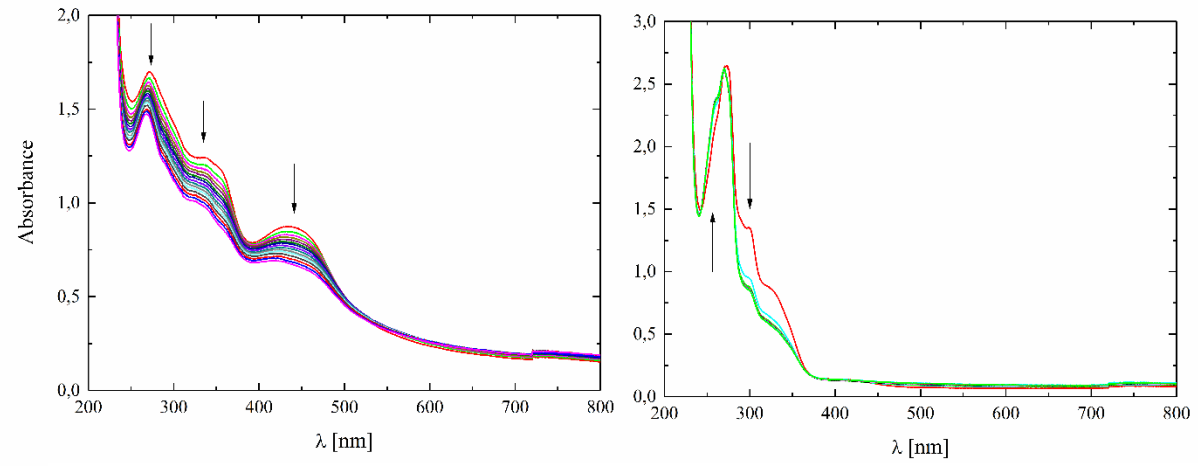

Figure 11. The electron spectra of **2** in DMSO-H_2O mixture (20µl + 3 ml) at pH = 7.00 (left) and 2.00 (right). T = 37°C, d = 1 cm, c = mol/dm^3, 15 spectra measured every 340s. The arrows indicate the direction of the changes

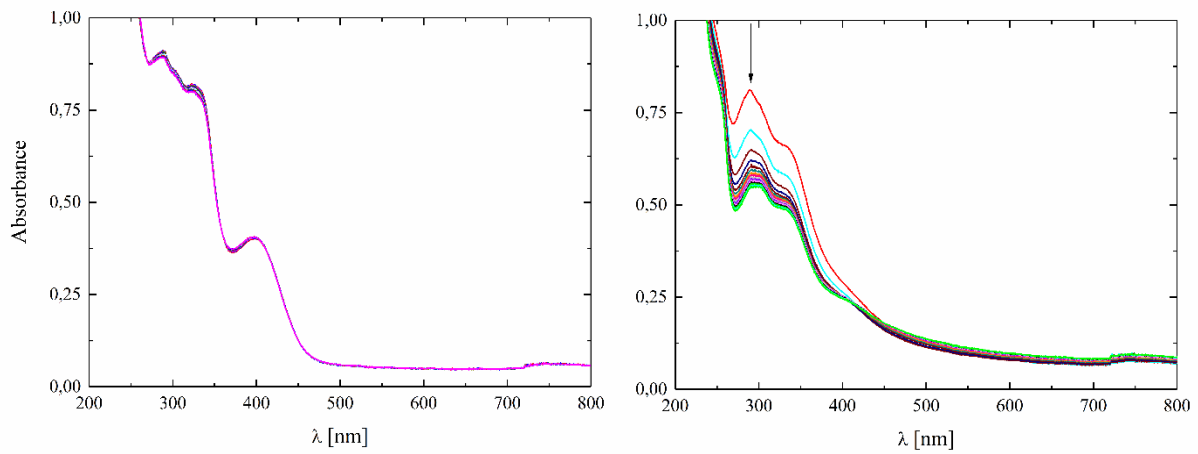

Figure 12. The electron spectra of **3** in DMSO-H_2O mixture (20µl + 3 ml) at pH = 7.00 (left) and 2.00 (right). T = 37°C, d = 1 cm, c = mol/dm^3, 15 spectra measured every 340s. The arrows indicate the direction of the changes

3. EPR spectrum

The EPR spectrum of complex **1** is presented in Fig. 13. Due to measured magnetic moment of 2.55 μ_B (calculated for V(I-II) 2.83 μ_B, for V(IV) 1.73 μ_B), it must be stressed, that **1** contains V(III), not visible in the EPR X-band, and only very small amounts of V(IV). The presence of this signal (Fig. 13) can be attributed to the small quantities of V(IV) formed by oxidation of complex **1**. The spectrum is a superposition of two signals which were simulated with the following parameters: center C1' $g_{\|}$ = 1.946, $A_{\|}$= 179.3 G, $g_{\perp}$ = 1.980, $A_{\perp}$ = 63.6 G and C2' $g_{\|}$ = 1.921, $A_{\|}$ = 180.9 G, $g_{\perp}$ = 1.979, $A_{\perp}$ = 69.8 G. The ^{51}V hyperfine coupling constant (179 for **1**) indicates, that V(IV) presents in **1** exists in V=O form, for the nonoxo V(IV) complexes the hyperfine coupling usually are lower than 130 G. [24]. This indicates, that oxidation of **1** results in ring opening and formation of oxido form.

Conclusions

Three new complexes of V(III), V(IV) and V(V) with tridentate ONO Schiff base ligands were synthesized and characterized. The X-ray single crystal structure of complex **3** indicates rare pure square pyramidal geometry of vanadium central atom. The EPR measurements show, that V(III) is contaminated with a small amount of V(IV) oxido complex, while most of the complex is of nonoxido type. The stability of the solutions indicate, that they can be used for cell culture media investigations, but in *in vivo* studies injections are recommended as complexes are relatively unstable at pH typical for digestion system.

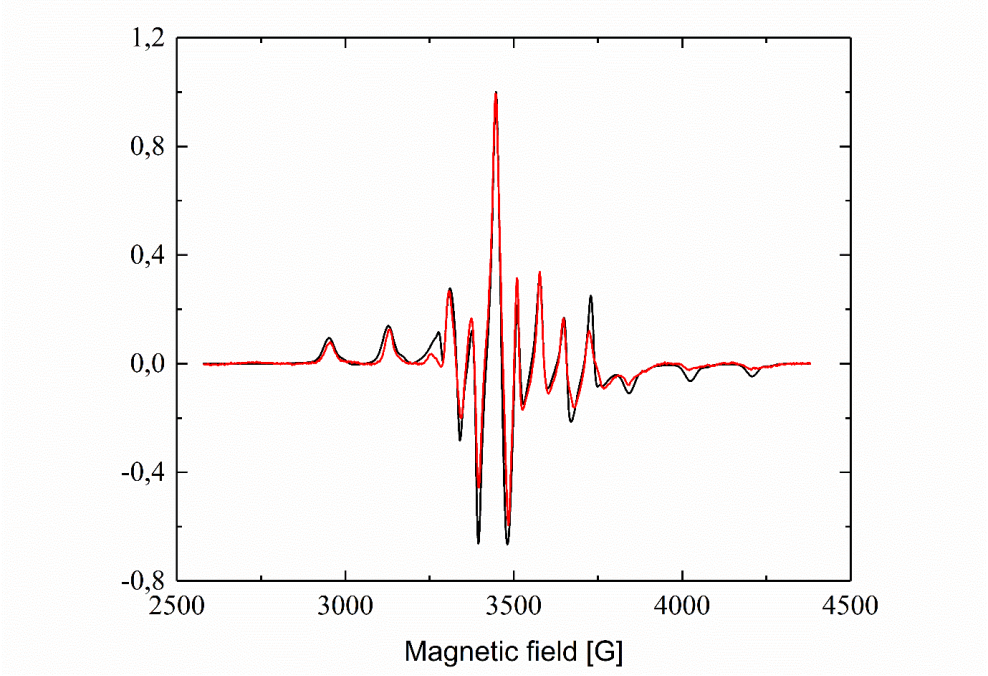

Figure 13. X-band EPR spectrum of complex **1** registered at RT. Black line: simulated spectra, red line: experimental spectra

Acknowledgments

This work was partly financed by the European Regional Development Fund under the Innovative Economy Programme 2007–2013 (WND POIG.01.03.01-174/09). The complexes are protected by the patent P.401493. We would like to thank to all persons from chemical team of the project for help in synthesis of the complexes.

References

1. Rehder D. Perspectives for vanadium in health issues. Future Medicinal Chemistry. 2016; 8:325-338.
2. Datta C, Das D, Mondal P, Chakraborty B, Sengupta M, Bhattacharjee CR. Novel water soluble neutral vanadium(I)--antibiotic complex: Antioxidant, immunomodulatory and molecular docking studies. European Journal of Medicinal Chemistry. 2015; 97:214-224.
3. Cransab DC, Trujillo AM, Pharazyn PS, Cohen MD. How environment affects drug activity: Localization, compartmentalization and reactions of a vanadium insulin-enhancing compound, dipicolinatooxovanadium(V). Coordination Chemistry Reviews. 2011; 255(19-20):2178-2192.
4. Poucheret P, Verma S, Grynpas MD, McNeill JH. Vanadium and diabetes. Molecular and Cellular Biochemistry. 1998; 188:73–80.
5. Rehder D. Structure and function of vanadium compounds in living organisms. Biometals. 1992; 5(1):3-12.
6. Doucette KA, Hassell KN, Crans DC. Selective speciation improves efficacy and lowers toxicity of platinum anticancer and vanadium antidiabetic drugs. Journal of Inorganic Biochemistry. 2016; 165:56-70.
7. Levina A, McLeod AI, Gasparini SJ, Nguyen A, De Silva WGM, Aitken JB, Harris HH, Glover C, Johannessen B, Lay PA. Reactivity and Speciation of Anti-Diabetic Vanadium Complexes in Whole Blood and Its Components: The Important Role of Red Blood Cells. Inorganic Chemistry. 2015; 54(16):7753-7766.
8. Thompson KH, Orvig C. Vanadium in diabetes: 100 years from Phase 0 to Phase I. Journal of Inorganic Biochemistry. 2006; 100(12):925-1935.
9. Abbasi Z, Salehi M, Khaleghian A, Kubicki M. Co(III), V(IV) and Cu(II) complexes of bidentate N,O-donor Schiff base ligands: Characterization, anticancer activities and metal oxide nanoparticles preparation via solid state thermal decomposition. Applied Organometallic Chemistry. 2018; 32:e4542.
10. Crans DC, Yang L, Haase A, Yang X. Health Benefits of Vanadium and Its Potential as an Anticancer Agent. Metal ions in life sciences. 2018; 18:251-279.
11. Rozzo C, Sanna D, Garribba E, Serra M, Cantara A, Palmieri G, Pisano M. Antitumoral effect of vanadium compounds in malignant melanoma cell lines. Journal of Inorganic Biochemistry. 2017;174:14-24.
12. Bishayee A Waghray A, Patel MA, Chatterjee M. Vanadium in the detection, prevention and treatment of cancer: The in vivo evidence. Cancer Letters. 2010; 294(1):1-12.
13. Irving E, Stoker AW. Vanadium Compounds as PTP Inhibitors. Molecules. 2017; 22(12):2269.
14. Bhanot S, Michoulas A, McNeill JH. Antihypertensive effects of vanadium compounds in hyperinsulinemic, hypertensive rats. Molecular and Cellular Biochemistry. 1995; 153(1-2):205-209.
15. Abdel-Rahman LH, Abu-Dief AM, Azza MB, Abdel-Mawgoud AH. Three novel Ni(II), VO(II) and Cr(III) mononuclear complexes encompassing potentially tridentate imine ligand: Synthesis, structural characterization, DNA interaction, antimicrobial evaluation and anticancer activity. Applied Organometallic Chemistry. 2017; 31(e3750):1-14.
16. Iyyam S, Sorimuthu P, Subramanian P, Kandaswamy M. A novel insulin mimetic vanadium–flavonol complex: Synthesis, characterization and in vivo evaluation in STZ-induced rats. European Journal of Medicinal Chemistry. 2013; 63:109-117.
17. Smith DM, Pickering RM, Lewith GT. A systematic review of vanadium oral supplements for glycaemic control in type 2 diabetes mellitus. QJM: An International Journal of Medicine. 2008; 101:351-358.
18. Spałek T, Pietrzyk P, Sojka Z. Application of the genetic algorithm joint with the Powell method to nonlinear least-squares fitting of powder EPR spectra. Journal of Chemical Information and Modeling. 2005; 45:18-29
19. Nonius COLLECT. Nonius BV, Delft, The Netherlands; 1998.
20. Otwinowski Z, Minor W., Processing of X-ray diffraction data collected in oscillation mode. Methods in Enzymology, Vol. 276, Macromolecular Crystallography, Part A, edited by Carter Jr CW, Sweet RM, New York: Academic Press; 1997. p. 307–326.
21. Sheldrick GM. Crystal structure refinement with SHELXL. Acta Crystallographica C Structural Chemistry. 2015; 71:3-8.
22. Brandenburg K, Putz H. DIAMOND. Crystal Impact GbR, Bonn, Germany; 2015.
23. Schilt AA, Taylor RC. Infra-red spectra of 1:10-phenanthroline metal complexes in the rock salt region below 2000 cm^{-1}. Journal of Inorganic and Nuclear Chemistry. 1959; 9:211-221.
24. Sanna D, Várnagy K, Lihi N, Micera G, Garribba E. Formation of New Non-oxido Vanadium(IV) Species in Aqueous Solution and in the Solid State by Tridentate (O, N, O) Ligands and Rationalization of Their EPR Behavior. Inorganic Chemistry. 2013; 52:8202-8213.